Available online at www.sciencedirect.com

ScienceDirect

Charm Mixing and *D* Dalitz Analysis at BESIII

Shengsen SUN (for the BESIII collaboration)

Institute of High Energy Physics, Beijing 100049, People's Republic of China

Abstract

We study $D^0\bar{D}^0$ pairs produced in e^+e^- collisions at $\sqrt{s}$ = 3.773 GeV using a data sample of $2.92\,fb^{-1}$ collected with the BESIII detector. Using world-average values of external parameters, we obtain $\cos\delta_{K\pi}$ = 1.02±0.11±0.06±0.01, $\delta_{K\pi}$ is the strong phase difference between the doubly Cabibbo-suppressed process $\bar{D}^0{\to}K^-\pi^+$ and the Cabibbo-favored process $D^0{\to}K^-\pi^+$. A measurement of the parameter y_{CP} in $D^0 - \bar{D}^0$ oscillations is performed by taking advantage of quantum coherence between pair-produced D^0 and $\bar{D}^0$ mesons near threshold, the preliminary result is y_{CP} = $(-1.6 \pm 1.3 \pm 0.6)\%$. An analysis of the $D^+{\to}K_S^0\pi^+\pi^0$ Dalitz plot is performed, the Dalitz plot is found to be well presented by a combination of six quasi-two-body decay channels $[K_S^0\rho^+, K_S^0\rho(1450)^+, \bar{K}^{*0}\pi^+, \bar{K}_0(1430)^0\pi^+, \bar{K}(1680)^0\pi^+, \bar{\kappa}^0\pi^+]$ plus a small nonresonant component. Using the fit fractions from this analysis, partial branching ratios are updated with higher precision than previous measurements.

Keywords: the BESIII detector, $D^0 - \bar{D}^0$ oscillation, strong phase difference, y_{CP}, Dalitz analysis

1. Introduction

Mixing of neutral mesons occurs when the flavor eigenstates differ from the physical mass eigenstates. In charm sector, $D^0 - \bar{D}^0$ mixing is a small effect in the Standard Model. While the short-distance effect is suppressed both by CKM matrix [1] and the GIM mechanism [2], charm mixing is expected to be dominated by long-distance process which make it difficult to be calculated reliably. To measure the charm mixing parameters helps to study the size of the long distance effect and search for new physics [3]. Many sophisticated experimental efforts have been made in the past decades, and these results indicate that D^0 and $\bar{D}^0$ do mix. Charm mixing is established by the LHCb [4] in 2013 and verified by the CDF [5] and Belle [6] experiment, subsequently.

Conventionally, charm mixing is described by two dimensionless parameters $x = 2\frac{M_1-M_2}{\Gamma_1+\Gamma_2}$ and $y = \frac{\Gamma_1-\Gamma_2}{\Gamma_1+\Gamma_2}$,

where $M_{1,2}$ and $\Gamma_{1,2}$ are the masses and widths of two mass eigenstates. The mass eigenstates of D which are linear combinations of flavor eigenstates are expressed as $|D_{1,2}\rangle = p|D^0\rangle + q|\bar{D}^0\rangle$, where p and q are complex parameters and they have phase difference ϕ. With the help of the conventions $CP|D^0\rangle = |\bar{D}^0\rangle$, CP eigenstates can be written as $|D_{CP+}\rangle \equiv \frac{|D^0\rangle+|\bar{D}^0\rangle}{\sqrt{2}}$ and $|D_{CP-}\rangle \equiv \frac{|D^0\rangle-|\bar{D}^0\rangle}{\sqrt{2}}$. The parameter y_{CP} can also be defined to express the differences between effective lifetime of D decays to CP eigenstates and flavor eigenstates. In the absence of direct CP violation, but allowing for small indirect CP violation [7], we have

$$y_{CP} = \frac{1}{2}[y\cos\phi(|\frac{q}{p}| + |\frac{p}{q}|) - x\sin\phi(|\frac{q}{p}| - |\frac{p}{q}|)]. \quad (1)$$

In case of no CPV, we have $|p/q| = 1$ and $\phi = 0$. Hence, $y_{CP} = y$.

So far, most of our knowledge about $D^0 - \bar{D}^0$ mixing are from time-dependent measurements. And the most precise determination of the size of the mixing are obtained by focusing on the time-dependent decay rate of the wrong-sign process $D^0{\to}K^+\pi^-$. These

Email address: sunss@ihep.ac.cn (Shengsen SUN (for the BESIII collaboration))

analyses are sensitive to $y' \equiv y\cos\delta_{K\pi} - x\sin\delta_{K\pi}$ and $x' \equiv x\cos\delta_{K\pi} + y\sin\delta_{K\pi}$ [4, 5, 8]. Where the $-\delta_{K\pi}$ is the relative strong phase between the doubly Cabibbo-suppressed (DCS) decay $D^0 \to K^+\pi^-$ and the corresponding Cabibbo-favored (CF) $\bar{D}^0 \to K^-\pi^+$

$$\frac{\langle K^-\pi^+|\bar{D}^0\rangle}{\langle K^-\pi^+|D^0\rangle} = -re^{-i\delta_{K\pi}}. \qquad (2)$$

Here, $r = \left|\frac{\langle K^-\pi^+|\bar{D}^0\rangle}{\langle K^-\pi^+|D^0\rangle}\right|$. The measurement of $\delta_{K\pi}$ can allow x and y to be extracted from x' and y'. Determination of $\delta_{K\pi}$ is important for this extraction. Furthermore, finer precision of $\delta_{K\pi}$ helps the γ/ϕ_3 angle measurement in CKM matrix according to the so-called ADS method [9]. In the limit of CP conservation, $\delta_{K^-\pi^+}$ is the same as $\delta_{K^+\pi^-}$. We use the notation of $K^-\pi^+$, and its charge conjugation mode is always implied to be included throughout the report.

At BESIII, $\delta_{K\pi}$ and y_{CP} can be determined using the time-independent measurements. In the mass-threshold production process $e^+e^- \to D^0\bar{D}^0$, the $D^0\bar{D}^0$ pair is in a state of definite $C = -$, because of the initial state (the virtual photon) has $J^{PC} = 1^{--}$. Thus the D^0 and $\bar{D}^0$ mesons are quantum-correlated. This provides an unique way to probe $D^0 - \bar{D}^0$ mixing as well as the strong phase differences between D^0 and $\bar{D}^0$ decays [10].

Three-body decays provide a rich laboratory in which to study the interferences between intermediate-state resonances. They also provide a direct probe of final-state interactions in certain decays. When a particle decays into three pseudo-scalar particles, intermediate resonances which dominate the decay rate and amplitudes are typically obtained with a Dalitz plot analysis technique [11]. This provides both the amplitudes and phases of the intermediate decay channels, which in turn allows us to deduce their relative branching fractions. These phase differences can even allow details about very broad resonances to be extracted by observing their interference with other intermediate states.

The previous Dalitz plot analysis of $D^+ \to K_S^0\pi^+\pi^0$ by MARKIII [12] included only two intermediate decay channels, $K_S^0\rho$ and $\bar{K}^{*0}\pi^+$, and was based on a small data set. With much larger statistics, it is possible to measure relative branching fractions more precisely and to find more intermediate resonances for BESIII.

A large contribution from a $K\pi$ S-wave intermediate state has been observed in earlier experiments. Both E791 [13][14] and CLEO-c [15] interpreted their data with a Model-Independent Partial Wave Analysis (MIP-WA) and found a phase shift at low $K\pi$ mass to confirm the $\kappa\pi$ component in the $D^+ \to K^-\pi^+\pi^+$ decay. Complementary to this channel, the $D^+ \to K_S^0\pi^+\pi^0$ decay

is also a golden channel to study the $K\pi$ S-wave in D decays.

In this report, we present the determination of $\delta_{K\pi}$ and preliminary result of y_{CP} by analysing coherent $D^0\bar{D}^0$ decays, and Dalitz plot analysis of $D^+ \to K_S^0\pi^+\pi^0$. These analyses are based on 2.92 fb^{-1} data at $\sqrt{s} = 3.773 GeV$ in e^+e^- collisions collected with the BESI-II detector. Details of the BESIII detector can be found elsewhere [16].

2. Measurement of the relative strong phase $\delta_{K\pi}$

With the assumption of CP conservation, the relative strong phase $\delta_{K\pi}$ can be accessed using these following formula [17] [18]

$$2r\cos\delta_{K\pi} + y = (1 + R_{WS}) \cdot \mathcal{A}_{CP\to K\pi}, \qquad (3)$$

$$\mathcal{A}_{CP\to K\pi} = \frac{\mathcal{B}_{D_{CP-}\to K\pi} - \mathcal{B}_{D_{CP+}\to K\pi}}{\mathcal{B}_{D_{CP-}\to K\pi} + \mathcal{B}_{D_{CP+}\to K\pi}} \qquad (4)$$

where R_{WS} is the decay rate ratio of the wrong sign process $\bar{D}^0 \to K\pi$ and the right sign process $D^0 \to K\pi$ and $\mathcal{B}$ denotes branching fractions. Benefiting from quantum-coherence, at BESIII, we can use CP tagging method to measure the branching fractions

$$\mathcal{B}_{D^{CP\mp}\to K\pi} = \frac{n_{K\pi,CP\pm}}{n_{CP\pm}} \cdot \frac{\varepsilon_{CP\pm}}{\varepsilon_{K\pi,CP\pm}}, \qquad (5)$$

In addition, most of systematic errors can be cancelled. Here, $n_{CP\pm}$ ($n_{K\pi,CP\pm}$) and $\varepsilon_{CP\pm}$ ($\varepsilon_{K\pi,CP\pm}$) are yields and detection efficiencies of single tags (ST) of $D\to CP\pm$ (double tags (DT) of $D^0\bar{D}^0\to CP\pm$; $K\pi$), respectively. With external inputs of the parameters of r, y and R_{WS}, one can extract $\delta_{K\pi}$.

In this analysis, 5 CP-even D^0 decay modes ($K^+K^-, \pi^+\pi^-, K_S^0\pi^0\pi^0, \pi^0\pi^0, \rho^0\pi^0$) and 3 CP-odd modes ($K_S^0\pi^0, K_S^0\eta, K_S^0\omega$) are used, with $\pi^0\to\gamma\gamma$, $\eta\to\gamma\gamma$, $K_S^0\to\pi^+\pi^-$ and $\omega\to\pi^+\pi^-\pi^0$. The key variable

$$M_{BC} \equiv \sqrt{E_0^2/c^4 - |\vec{p}_D|^2/c^2} \qquad (6)$$

is used to identify signals. Here $\vec{p}_D$ is the total momentum of the D^0 candidate and E_0 is the beam energy. Maximum likelihood fits are performed to M_{BC} distribution to get yields of the CP ST signals. Signals are modeled using the shape derived from MC simulation convoluted with a smearing Gaussian function, and backgrounds are described by the ARGUS function [19]. In the events of the CP ST modes, the $K\pi$ combinations are reconstructed using the remaining charged tracks with respect to the ST D candidates. Similar fits are performed to the distributions of $M_{BC}(D\to CP\pm)$ in the survived DT events to estimate yields of DT signals. These fits are shown in Fig. 1.
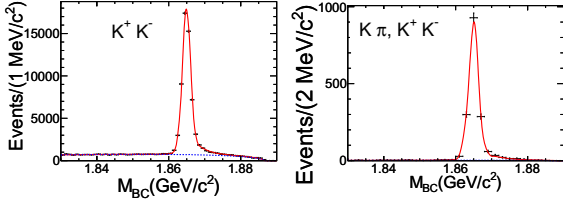
(a) ST M_{BC} fit of the $D{\rightarrow}K^+K^-$ (b) DT M_{BC} fit of the $K^+K^-; K\pi$

Figure 1: In both figures, data are shown in points with error bars. The solid red lines show the total fits and the dashed blue lines show the background shapes.

(a) U_{miss} fit for CP-tagged $Ke\nu$ (b) U_{miss} fit for CP-tagged $K\mu\nu$

Figure 2: U_{miss} distributions and fits to data.

We get $\mathcal{A}_{CP\rightarrow K\pi} = (12.7 \pm 1.3 \pm 0.7)\%$, where the first uncertainty is statistical and the second is systematic. To measure the strong phase $\delta_{K\pi}$ in Eq. 3, we quote the external inputs of $R_{\text{D}} = r^2 = (3.47 \pm 0.06)\text{‰}$, $y = (6.6 \pm 0.9)\text{‰}$, and $R_{\text{WS}} = (3.80 \pm 0.05)\text{‰}$ from HFAG 2013 [20] and PDG [7]. Finally, we obtain $\cos \delta_{K\pi} = 1.02 \pm 0.11 \pm 0.06 \pm 0.01$, where the first uncertainty is statistical, the second uncertainty is systematic, and the third uncertainty is due to the errors introduced by the external input parameters. This result is more precise than CLEO's measurement [17, 20] and provides the world best constrain on $\delta_{K\pi}$.

3. Measurement of y_{CP}

y_{CP} can be extracted by the semileptonic decays of $D^0 \rightarrow l$ using the following equation [18]
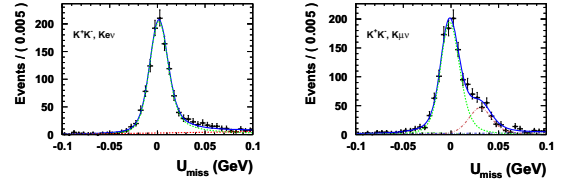
$$y_{\text{CP}} = \frac{1}{4}\left(\frac{\mathcal{B}_{D_{CP-}\rightarrow l}}{\mathcal{B}_{D_{CP+}\rightarrow l}} - \frac{\mathcal{B}_{D_{CP+}\rightarrow l}}{\mathcal{B}_{D_{CP-}\rightarrow l}}\right), \quad (7)$$

where the branching ratios $\mathcal{B}_{CP\mp}$ can be obtained by

$$\mathcal{B}_{CP\mp} = \frac{n_{l;CP\pm}}{n_{CP\pm}} \cdot \frac{\varepsilon_{CP\pm}}{\varepsilon_{l;\,CP\pm}}. \quad (8)$$

To combine results from different tag modes, we determine y_{CP} using $\tilde{\mathcal{B}}_\pm$ which is obtained from $\chi^2 = \sum_\alpha \frac{(\tilde{\mathcal{B}}_\pm - \mathcal{B}_\pm^\alpha)^2}{(\sigma_\pm^\alpha)^2}$. Here, α denotes different CP-tag modes. 3 CP-even tag modes (K^+K^-, $\pi^+\pi^-$, $K_S\pi^0\pi^0$) and 3 CP-odd tag modes ($K_S^0\pi^0$, $K_S^0\omega$, $K_S^0\eta$)are used in this analysis. Similar to the analysis of $\delta_{K\pi}$, ST yields are estimated by fitting to the M_{BC} distributions. Semileptonic decays of $D{\rightarrow}Ke\nu$ and $D{\rightarrow}K\mu\nu$ are reconstructed with respect to the CP-tagged D candidates in ST events. These reconstruction are partial reconstruction due to the undetectable neutrino in the final states. Variable U_{miss} is defined to distinguish the semileptonic signals from backgrounds

$$U_{\text{miss}} \equiv E_{\text{miss}} - |\vec{p}_{\text{miss}}|, \quad (9)$$

$$E_{\text{miss}} \equiv E_0 - E_K - E_l, \quad (10)$$

$$\vec{p}_{\text{miss}} \equiv -[\vec{p}_K + \vec{p}_l + \hat{p}_{\text{ST}} \sqrt{E_0^2 - m_D^2}]. \quad (11)$$

Here, $E_{K/l}$ ($\vec{p}_{K/l}$) is the energy (three-momentum) of $K^\pm$ or lepton $l^\mp$, $\hat{p}_{\text{ST}}$ is the unit vector in the reconstructed direction of the CP-tagged D and m_D is the nominal D^0 mass. U_{miss} of correctly-reconstructed signals should peaks at zero. U_{miss} fit plots are shown in Fig. 2.

In the U_{miss} fitting, for $Ke\nu$ mode, signal shape is modeled using MC shape convoluted with an asymmetric Gaussian and backgrounds are described with a 1st-order polynomial function. For $K\mu\nu$ mode, signal shape is modeled using MC shape convoluted with an asymmetric Gaussian. Backgrounds of $Ke\nu$ are modeled using MC shape and their relative rate to the signals are fixed. Shape of $K\pi\pi^0$ backgrounds are taken from MC simulations with convolution of a smearing Gaussian function; parameters of the smearing function are fixed according to fits to the control sample of $D{\rightarrow}K\pi\pi^0$ events. Size of $K\pi\pi^0$ backgrounds are fixed by scaling the number of $K\pi\pi^0$ events in the control sample to the number in the signal region according to the ratio estimated from MC simulations. Other backgrounds are described with a 1st-order polynomial function. Finally, we obtain the preliminary result as $y_{\text{CP}} = (-1.6 \pm 1.3 \pm 0.6)\%$, where the first uncertainty is statistical, the second uncertainty is systematic. The result is compatible with the previous measurements [20]. This is the most precise measurement of y_{CP} based on $D^0\bar{D}^0$ threshold productions. However, its precision is still statistically limited.

4. Dalitz Plot Analysis of $D^+ \rightarrow K_S^0\pi^+\pi^0$

The likelihood function is defined as $\mathcal{L} = \prod_{i=1}^{N} \mathcal{P}(x_i, y_i)$, where N is the event number and $\mathcal{P}(x, y)$ is the probability density function on Dalitz plot. For

signal with background in data, it is described as

$$\mathcal{P}(x,y) = f_S \frac{|\mathcal{M}(x,y)|^2 \varepsilon(x,y)}{\int\limits_{DP} |\mathcal{M}(x,y)|^2 \varepsilon(x,y) dx dy}$$

$$+ f_B \frac{B(x,y)}{\int\limits_{DP} B(x,y) dx dy}, \qquad (12)$$

where $\mathcal{M}(x,y)$ is the decay matrix element, $\varepsilon(x,y)$ is the efficiency shape, $B(x,y)$ is the background shape, f_S and f_B are the fractions of signal and background, respectively. The DP denotes the kinematic limit on the Dalitz ploy. The decay matrix element is contributed by isobar model. The efficiency is parameterized by Monte-Carlo sample [21]. The background includes two parts: peaking background and non-peaking background. The peaking background is estimated by Monte-Carlo simulation, and the non-peaking background is parameterized by the low and high sidebands of the distribution of the recoiling mass of selected D meson m_{rec} of data. The fractions of signal and background are fitted by the distribution of the m_{rec}.

Based on 166,694 selected candidate events with a background of 15.1%, a decay matrix element is constructed by possible intermediate resonance decay modes. After more possible intermediate resonance decay modes were considered in different isobar models, three models are compared principally, the Cabbibo favored model, the model without the $\bar{\kappa}$ and the model without the non-resonant. The results are listed in the column "Favored", "w/o $\bar{\kappa}$"and "w/o NR"of Table 1, respectively. It is found that the goodness of fit in the "w/o $\bar{\kappa}$"model is much worse than in the favored model, which indicates the $\bar{\kappa}$ has a large confidence level in our data. If a non-resonant component is removed, the goodness of fit also becomes worse, indicating the non-resonant is indeed present in our data.

In the above three models, the contributions of the three channels $\bar{K}^*(1410)^0\pi^+$, $\bar{K}_2^*(1430)^0\pi^+$ and $\bar{K}_3^*(1780)^0\pi^+$ are not significant, and their fit fractions are less than 0.2%. Therefore, we remove them from the final model. The final model (F) is composed of a non-resonant component and intermediate resonances modes, including $K_S^0\rho(770)^+$, $K_S^0\rho(1450)^+$, $\bar{K}^*(892)^0\pi^+$, $\bar{K}_0^*(1430)^0\pi^+$, $\bar{K}^*(1680)^0\pi^+$ and $\bar{\kappa}^0\pi^+$. The projections of the fit and the Dalitz plot can be found in Fig. 3.

A deviation of efficiency between data and MC simulation will cause a deviation of the fit results. Therefore, a momentum-dependent correction is applied to the final results. The results are listed in the column "Final"of Table 1.
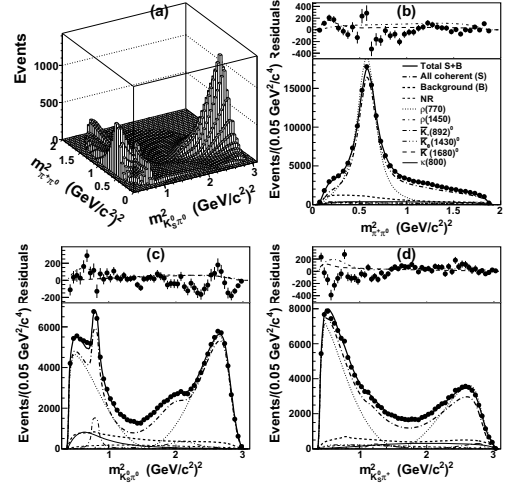

Figure 3: The results of fitting the $D^+ \rightarrow K_S^0 \pi^+ \pi^0$ data with final chosen resonances. (a) Distribution of fitted p.d.f. and projections on (b) $m_{\pi^+\pi^0}^2$, (c) $m_{K_S^0\pi^0}^2$ and (d) $m_{K_S^0\pi^+}^2$. Residuals between data and the total p.d.f. are shown by dots with statistical error bars on the top insets.

In fits with these models, the formalism of the κ is taken as the complex pole form, and the position of the pole κ is allowed to float as a free complex parameter. The mass and width of the $K_0^*(1430)^0$, taken as a Breit-Wigner function, are also floated, since the measured values from E791 [13] and CLEO-c [15] in the $D^+ \rightarrow K^-\pi^+\pi^+$ decay are not consistent with the PDG ones. Finally, the pole of the κ obtained is at $(752 \pm 15 \pm 69^{+55}_{-73}, -229 \pm 21 \pm 44^{+40}_{-55})$ MeV, which is consistent with the model C result of CLEO-c. And the mass and width of the $K_0^*(1430)^0$ are $1464 \pm 6 \pm 9^{+9}_{-28}$ MeV and $190 \pm 7 \pm 11^{+6}_{-26}$ MeV, respectively, and are consistent with CLEO-c's results, while they are not consistent with the PDG. In the model without the $\bar{\kappa}$, the results are 1444 ± 4 MeV and 283 ± 11 MeV with statistical errors only, which are consistent with the PDG values.

5. Summary

With the 2.92 fb^{-1} e^+e^- collision data collected with the BESIII detector at $\sqrt{s} = 3.773$GeV, we obtain the strong phase difference $\cos\delta_{K\pi}$ in $D{\rightarrow}K\pi$ decays and the mixing parameter y_{CP}. Using the same data sample, a Dalitz analysis of the decay $D^+ \rightarrow K_S^0\pi^+\pi^0$ is performed. We fit the distribution of data to a coherent sum of six intermediate resonances plus a nonresonant component, with a low mass scalar meson, the $\bar{\kappa}$, included. These measurements were carried out based on the quantum-correlated technique. The preliminary results are given as $\cos\delta_{K\pi} = 1.02 \pm 0.11 \pm 0.06 \pm 0.01$

Decay Mode	Parameters	Favored	w/o $\bar{\kappa}$	w/o NR	Final
Non-resonant	FF(%)	4.5±0.7	18.3±0.6		4.6±0.7
	$\phi(°)$	269±6	232.7±1.3		279±6
$K_S^0\rho(770)^+$	FF(%)	84.6±1.8	82.0±1.3	86.7±1.1	83.4±2.2
	$\phi(°)$	0(fixed)	0(fixed)	0(fixed)	0(fixed)
$K_S^0\rho(1450)^+$	FF(%)	1.80±0.20	6.03±0.29	0.63±0.12	2.13±0.22
	$\phi(°)$	198±4	167.1±2.1	186±8	187.0±2.6
$\bar{K}^*(892)^0\pi^+$	FF(%)	3.22±0.14	2.99±0.10	3.30±0.10	3.58±0.17
	$\phi(°)$	294.7±1.3	279.3±1.2	292.3±1.5	293.2±1.3
$\bar{K}^*(1410)^0\pi^+$	FF(%)	0.12±0.05	0.18±0.05	0.12±0.05	
	$\phi(°)$	228±9	301±10	243±12	
$\bar{K}_0^*(1430)^0\pi^+$	FF(%)	4.5±0.6	10.5±1.3	3.6±0.5	3.7±0.6
	$\phi(°)$	319±5	306.2±2.0	317±4	334±5
$\bar{K}_2^*(1430)^0\pi^+$	FF(%)	0.118±0.018	0.086±0.014	0.111±0.015	
	$\phi(°)$	273±7	265±9	267±7	
$\bar{K}^*(1680)^0\pi^+$	FF(%)	0.21±0.06	0.58±0.08	0.43±0.10	1.27±0.11
	$\phi(°)$	243±6	284±4	234±5	251.8±1.9
$\bar{K}_3^*(1780)^0\pi^+$	FF(%)	0.034±0.008	0.055±0.008	0.037±0.008	
	$\phi(°)$	130±12	113±9	131±11	
$\bar{\kappa}^0\pi^+$	FF(%)	6.8±0.7		18.8±0.5	7.7±1.2
	$\phi(°)$	92±6		11.6±1.9	93±7
NR+$\bar{\kappa}^0\pi^+$	FF(%)	18.1±1.4	18.3±0.6	18.8±0.5	19.2±1.8
$K_S^0\pi^0$ S wave	FF(%)	18.9±1.0	15.8±1.0	21.2±1.0	17.1±1.4
χ^2/n		1672/1209	2497/1209	1777/1209	2068/1209

Table 1: The preliminary results of the fits to the $D^+ \to K_S^0\pi^+\pi^0$ Dalitz plot with statistical errors only for different resonance choices, fit fraction (FF) and phase (ϕ). The "Final"are momoentum-dependent corrected.

and $y_{\rm CP} = (-1.6 \pm 1.3 \pm 0.6)\%$. The measurement of $\delta_{K\pi}$ is the most precise to date. The result of $\cos\delta_{K\pi}$ is the most accurate to date. In the future, global fits can be implemented in order to best exploit BESIII data in the quantum-coherence productions [22]. The $D^+ \to K_S^0\pi^+\pi^0$ Dalitz plot is well-represented by a combination of a non-resonant component plus six quasi-two-body decays, $\bar{\kappa}$ included. The results are consistent with the results of the E791 and CLEO-c collaboration for the $D^+ \to K^-\pi^+\pi^+$ decay. The final fit fraction and phase for each component, multiplied by the world average $D^+ \to K_S^0\pi^+\pi^0$ branching ratio of $(6.99\pm0.27)\%$ [7], which yield the partial branching fractions shown in Table 2. The error on the world average branching ratio is incorporated by adding it in quadrature with the experimental systematic errors on the fit fractions to give the experimental systematic error on the partial branching fractions. The $K_S^0\pi^0$ waves in the $D^+ \to K_S^0\pi^+\pi^0$ decay can be compared with the $K^-\pi^+$ waves in the $D^0 \to K^-\pi^+\pi^+$ decay, which is consistent with the expectation.

References

[1] Cabibbo, Nicola, Phys. Rev. Lett. **10** (1963) 531;
M. Kobayashi and T. Maskawa, Prog. Theor. Phys. **49** (1973) 652.

[2] S. L. Glashow, J. Illiopoulos, and L. Maiani, Phys. Rev. D **2** (1970) 1285.

[3] S. Bianco, F. L. Fabbri, D. Benson and I. Bigi, Riv. Nuovo Cim. **26**(7) (2003) 1.

[4] R. Aaij *et al.* [LHCb Collaboration], arXiv:1309.6534 [hep-ex];
R. Aaij *et al.* [LHCb Collaboration], Phys. Lett. **110** (2013) 101802.

[5] T. Aaltonen *et al.* [CDF Collaboration], Phys. Rev. Lett. **111** (2013) 231802.

[6] B. Ko *et al.* [Belle Collaboration], Phys. Rev. Lett. **112** (2014) 111801.

[7] J. Beringer *et al.* [Particle Data Group], Phys. Rev. D **86** (2012) 010001.

[8] M. Staric *et al.* [Belle Collaboration], arXiv:1212.3478 [hep-ex];
P.del Amo Sanchez *et al.* [BaBar Collaboration], Phys. Rev. Lett. **105** (2010) 081803.

[9] David Atwood, Isard Dunietz and Amarjit Soni, Phys. Rev. Lett. **78** (1997) 3257.

[10] X.-D. Cheng *et al.*, Phys. Rev. D **75** (2007) 094019.

Mode	Partial Branching Fraction (%)
$D^+ \to K_S^0 \pi^+ \pi^0$ Non Resonant	$0.32 \pm 0.05 \pm 0.25^{+0.28}_{-0.25}$
$D^+ \to \rho^+ K_S^0, \rho^+ \to \pi^+ \pi^0$	$5.83 \pm 0.16 \pm 0.30^{+0.45}_{-0.15}$
$D^+ \to \rho(1450)^+ K_S^0, \rho(1450)^+ \to \pi^+ \pi^0$	$0.15 \pm 0.02 \pm 0.09^{+0.07}_{-0.11}$
$D^+ \to \bar{K}^*(892)^0 \pi^+, \bar{K}^*(892)^0 \to K_S^0 \pi^0$	$0.250 \pm 0.012 \pm 0.015^{+0.025}_{-0.024}$
$D^+ \to \bar{K}_0^*(1430)^0 \pi^+, \bar{K}_0^*(1430)^0 \to K_S^0 \pi^0$	$0.26 \pm 0.04 \pm 0.05 \pm 0.06$
$D^+ \to \bar{K}^*(1680)^0 \pi^+, \bar{K}^*(1680)^0 \to K_S^0 \pi^0$	$0.09 \pm 0.01 \pm 0.05^{+0.04}_{-0.08}$
$D^+ \to \bar{\kappa}^0 \pi^+, \bar{\kappa}^0 \to K_S^0 \pi^0$	$0.54 \pm 0.09 \pm 0.28^{+0.36}_{-0.19}$
$NR + \bar{\kappa}^0 \pi^+$	$1.30 \pm 0.12 \pm 0.12^{+0.12}_{-0.30}$
$K_S^0 \pi^0$ S-wave	$1.21 \pm 0.10 \pm 0.16^{+0.19}_{-0.27}$

Table 2: The preliminary results of partial branching fractions calculated by combining our fit fractions with the PDG's $D^+ \to K_S^0 \pi^+ \pi^0$ branching ratio. The errors shown are statistical, experimental systematic and modeling systematic ones, respectively.

[11] R. H. Dalitz, Phil. Mag. **44**(1953) 1068.
[12] J. Adler *et al.* (MARK-III Collaboration), Phys. Lett. B **196** (1987) 107.
[13] E.M. Aitala *et al.* (E791 Collaboration), Phys. Rev. Lett. **89** (2002) 121801.
[14] E.M. Aitala *et al.* (E791 Collaboration), Phys. Rev. D **73** (2006) 032004.
[15] G. Bonvicini *et al.* (CLEO Collaboration), Phys. Rev. D **78** (2008) 052001.
[16] M. Ablikim *et al.* [BESIII Collaboration], Nucl. Instrum. Meth. A **614** (2010) 345.
[17] D. M. Asner *et al.* [CLEO Collaboration], Phys. Rev. D **78** (2008) 012001;
D. M. Asner *et al.* [CLEO Collaboration], Phys. Rev. D **86** (2012) 112001.
[18] Z.-Z. Xing, Phys. Rev. D **55** (1997) 196.
[19] H. Albrecht *et al.* [ARGUS Collaboration], Phys. Lett. B **241** (1990) 278.
[20] Heavy Flavor Averaging Group: http://www.slac.stanford.edu/xorg/hfag/charm/.
[21] W. D. Li, H. M. Liu *et al.*, in proceedings of CHEP06
[22] Y. Guan, X.-R. Lu, Y. Zheng and Y.-S. Zhu, Chinese Phys. C **37** (2013) 106201 [arXiv:1304.6170 [hep-ex]].